



Multi-proxy signatures in deep-water fine-grained sediments: Inherited versus syn-sedimentary factors controlling sediment compositions within a foredeep basin (Paleogene Adriatic foredeep – Northern Italy)

Andrea Di Capua^{a,b,*}, Samuele Miano^b, Davide Campagnolo^b, Sergio Bonomo^c, Antonio Caruso^d, Gabriele Carugati^b, Alessandro Cavallo^e, Franz A. Livio^b, Giovanni Vezzoli^e

^a CNR – Istituto di Geologia Ambientale e Geoingegneria, Via Mario Bianco 9, 20131, Milano, Italy

^b Università Degli Studi Dell'Insubria, Dipartimento di Scienza Ed Alta Tecnologia, Via Valleggio 11, 22100, Como, Italy

^c CNR – Istituto di Geologia Ambientale e Geoingegneria (CNR-IGAG), Area Della Ricerca di Roma 1- Strada Provinciale 35d, 9-00010, Montelibretti, Italy

^d Università Degli Studi di Palermo, Dipartimento di Scienze Della Terra e Del Mare, Via Archirafi 22, 90123, Palermo, Italy

^e Università Degli Studi di Milano - Bicocca, Centro Provenance, Dipartimento di Scienze Dell'Ambiente e Della Terra, Piazza Della Scienza 4, 20126, Milano, Italy

ARTICLE INFO

Keywords:

Provenance
Collisional belt
Paleo-drainages
Climate

ABSTRACT

This work explores the significance of sedimentary proxies recorded within the Paleogene fine-grained detritus of the Adriatic foredeep (Northern Italy). Such sequences represent the only sedimentary record describing the source-to-sink system delivering detritus from the growing Alpine belt to the basin during the Eocene – Oligocene boundary. The combination of x-ray powder diffractometric, petrographic, SEM-EDS and biostratigraphic analyses on more than twenty samples from the Ternate-Travedona Formation, the Chiasso Formation, and the Villa Olmo Conglomerate allowed to identify the source areas of detritus and potential fluvial paleo-drainages, possibly ascribable to two different sectors of the Southalpine domain. Comparison between these results and the petrographic composition of the Cretaceous wedge in the same area opens to the possibility that Cenozoic drainages were inherited from more limited paleo-drainages developed during the end of the Mesozoic. Results of provenance analysis also gives new insights on how detrital compositions may vary in function of grain-size in tropical-subtropical environments.

1. Introduction

Sediment provenance is a fundamental tool in the reconstruction of factors contributing to shaping Earth surface and driving the accumulation of detritus within depocenters through time (e.g., Garzanti, 2019 and ref. therein). In modern geology, sediment provenance is overall gain from consolidated methodologies on sands/sandstones (see Garzanti, 2019 for a complete review of the topic), and minorly on gravel-size detritus (e.g., DeCelles, 1988; Carrapa and Di Giulio, 2001; Di Capua et al., 2016a,b, 2022; Litty and Schlunegger, 2017). On the contrary, muddy (<62.5 μm) detritus always represented the Cinderella of clastic sediments, receiving the deserved attention for provenance studies only in the last decades (e.g., Caracciolo et al., 2009, 2020; Perri et al., 2012; Andò and Garzanti, 2014; Di Capua et al., 2016a, b; Borromeo et al., 2019; Paleari et al., 2019; Cavalcante et al., 2023). This unintentional overlook created a gap in the knowledge on the

relationship between provenance and geodynamics in sedimentary basins dominated by fine-grained sedimentation, such as in those surrounding the Alpine belt. There, in fact, sandy and gravel-sized detritus have been widely used for the identification of morphogenic steps in the evolution of the belt through sediment signatures since the upper Oligocene (post-collisional stage; e.g., Carrapa and Di Giulio, 2001; Di Giulio et al., 2001; Garzanti and Malusà, 2008; Malusà et al., 2011; Di Capua et al., 2016a, 2022; Lu et al., 2019), whereas the thick sequences of fine-grained sediments accumulated from the Eocene to the lower Oligocene (collisional stage) have always simply considered as a signal of low sediment production in response to the limited belt morphogenic growth during that period (Garzanti and Malusà, 2008).

The aim of this study is to investigate the sedimentary signatures within those fine-grained sedimentary sequences, considering them as fundamental in the comprehension of how the source-to-sink system comprised between the Periadriatic Fault system and the Adriatic

* Corresponding author. CNR – Istituto di Geologia Ambientale e Geoingegneria, Via Mario Bianco 9, 20131, Milano, Italy.

E-mail address: andrea.dicapua@igag.cnr.it (A. Di Capua).

foredeep evolved during the transition from non-collisional to collisional stages. Through a multidisciplinary approach based on petrographic, minero-chemical, and biostratigraphic analyses, it has been identified a double signature within the basin, inherited from the non-collisional paleo-drainage settings within the Southalpine domain during the Cretaceous. Throughout the comparison of fine-grained with sandy and gravel-sized detritus, it has been recognized a grain-size control on sediment composition, strongly influenced by paleo-

climatic conditions at which terranes were weathered and sediments were transported during the Paleogene. Such conditions were common across the Southalpine area (e.g., Bosellini and Trevisan, 1992), and influenced mineralogical composition of sediments along the Southern Alpine foreland basin (e.g., Aldega et al.). In addition, pulses of carbonate and clay minerals in fine-grained detritus may also indicate a local change in climate at the Rupelian/Chattian boundary. Finally, the absence of volcanogenic detritus across all the Paleogene time testifies

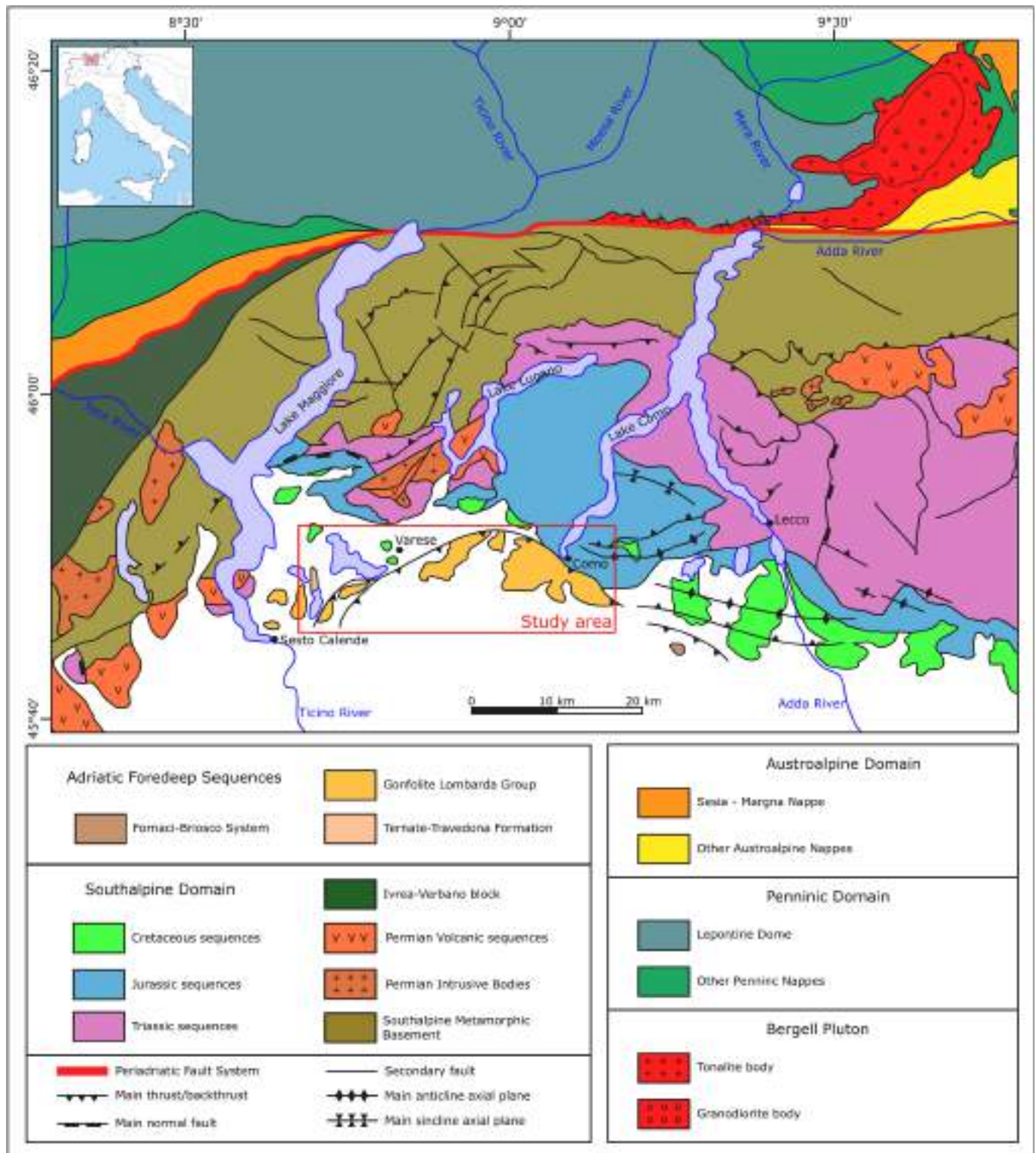


Fig. 1. Geological map of the Alps – Adriatic foredeep systems, modified from Di Capua et al. (2022).

the absence of drainages supplying Periadriatic volcanic centres' detritus to the Adriatic foredeep.

2. Geological background

The term “Adriatic foredeep basin” here indicates a foredeep depocenter developed south of the Southern Alps that received sediments' inputs from the central/western Alpine belt during the Paleogene and Neogene times. Some authors include it in the wider Southern Alpine foreland basin (e.g., Lu et al., 2020). The sedimentary record of the Adriatic foredeep basin is dominated, but not limited to, by clastic inputs deriving from the dismantling of the belt during different stages (e.g., Zanchetta et al., 2015; Garzanti and Malusà, 2008). It also includes bioclastic sequences deriving from the progradation of Paleogene carbonate platforms until the Rupelian (early Oligocene) (e.g., Mancin et al., 2001; Bini et al., 2015; Coletti et al., 2016), as well as minor volcanoclastic inputs during the Lutetian and Bartonian (middle Eocene) probably supplied by local eruptive centres (Gavazzi et al., 2003; Premoli Silva et al., 2010; Bini et al., 2015; Di Capua et al., 2021; Sciunnach, 2014). The present study takes into consideration two formations and one member accumulated during the Eocene – Oligocene boundary: the Ternate-Travedona Formation, the Chiasso Formation and the Villa Olmo Conglomerate (lower member of the Como Conglomerate Fm.; Figs. 1 and 2).

2.1. Ternate-Travedona Formation

The Ternate-Travedona Formation is a submarine apron developed during the accretion of a Paleogene calcareous platform (Mancin et al., 2001, Fig. 2). Nowadays, this platform does not exist anymore, completely unroofed and eroded during the Oligocene and Neogene Alpine orogenesis and accumulated as detritus within the sequences of the Gonfolite Lombarda Group (Sciunnach, 2014; Coletti et al., 2016). The apron hosts thick bioclastic limestones interbedded with thin marly layers (Bernoulli et al., 1988; Mancin et al., 2001; Coletti et al., 2016). Detrital signature of rare gravel-size particles within the bioclastic beds points to a detrital provenance from the Mesozoic Southalpine sequences (Bernoulli et al., 1988).

2.2. Lower Gonfolite Lombarda Group: Chiasso Formation and Villa Olmo Conglomerate

The Gonfolite Lombarda Group is a clastic submarine wedge divided into 15 Formations that accumulated from the Oligocene to the Late Miocene (Cita, 1957; Gelati et al., 1988; Bernoulli et al., 1993; Tremolada et al., 2010). It partially crops out between the towns of Como and Sesto Calende, buried below the Plio-Quaternary sediments of the Po Plain, to the South (Bersezio et al., 1993). The lowermost Formation,

named Chiasso Formation, probably began its accumulation interdigitating the Ternate-Travedona Formation apron in its uppermost part (Di Giulio et al., 2001; Coletti et al., 2016, Fig. 2). Tremolada et al. (2010) fix the beginning of the accumulation of the Chiasso Formation in Como at least at 31.4 Ma, considering that its base was tectonically removed by the Monte Olimpino backthrust, rooted at this stratigraphic unit. To the top, the Chiasso Formation interdigitates with the base of the Como Conglomerate (27.6 – ca. 23 Ma; Fig. 2). The Como Conglomerate is a thick, mainly gravelly sized Formation composed of two different members: the Villa Olmo Conglomerate (27.8–26.6 Ma) and the Camerlata Member (26.6 – ca. 23 Ma) (Tremolada et al., 2010). The present study is focused on the Villa Olmo Conglomerate. This member includes the first incoming of coarse-grained sediments into the Adriatic Foredeep generated by the dismantling of Southalpine terranes, Cenozoic plutonic bodies intruded on the Periadriatic Fault System (PFS), known as Bergell Pluton, and the surrounding metamorphic terranes of the Penninic terranes (Fig. 1) (Carrapa and Di Giulio, 2001; Di Giulio et al., 2001; Garzanti and Malusà, 2008; Di Capua et al., 2016a, 2022).

3. Methodology

Twenty-two samples have been collected along four different sections across the Italian-Swiss boundary between the town of Como and Varese (Northern Italy – Fig. 1). All the samples have been split up into sub-samples for a multidisciplinary investigation on each of them.

First, they were powdered and analysed through a Siemens D5000 powder XRD (Siemens, Karlsruhe, Germany) with a Bragg-Brentano θ - 2θ geometry. It was equipped with a Cu anode X-ray tube, which operated at 40 kV and 40 mA (radiation Cu-K α = 1.5406 Å), and a diffracted-beam graphite monochromator. A step size of 0.02° 2θ and a counting time of 1 s/step were found to give optimum results in terms of time per scan and peak resolution. The XRD patterns were collected in angular range between 2° and 62° at 2θ . The qualitative phase analysis was performed using the PANalytical HighScore Plus software version 2.2c using the ICSD PDF2-2008 database; quantitative phase analysis was carried out running the FULLPAT software (Chiperu and Bish, 2002).

Six of those samples have been also cut into standard thin sections and analysed under a polarized microscope to identify potential rock fragments driven the XRD signals (Table 1).

The chemical composition of a sample (oxide and sulfur components) has been verified using an environmental scanning electron microscope (ESEM FEG XL30, Philips, Eindhoven, The Netherlands) coupled with an X-ray energy dispersive spectrometer (EDAX AMETEK Element).

Analyses of foraminifera and calcareous nannofossils were carried out on them using a stereo microscope and a polarized light microscope (1000 ×) respectively in order to recognize the bioevents. For the calcareous nannofossil analyses standard rippled smear slides were prepared, without any chemical treatment, sieving or centrifuging. Separate analyses were also performed to evaluate the abundance of reworked specimens, which included taxa from different stratigraphic intervals (e.g., Cretaceous taxa). Calcareous nannofossil taxa were determined using the taxonomy proposed by Perch-Nielsen (1985) and Bown et al. (2004) and following the biostratigraphic scheme of Martini (1971) and Okada and Bukry (1980). For the foraminifera analyses 50 g of dried sediment were washed through a 63 μ m sieve and the residual fraction was oven-dried at 50 °C. The identification of the foraminiferal bio-events was based on a semi-quantitative study of the fraction greater than 125 μ m following the biostratigraphic scheme and taxonomy proposed by Bolli and Saunders (1985).

Finally, a single sample of sandstone, recovered within the Chiasso Formation in Como (Fig. 3B – MO1 sample), has been point-counted following the Gazzi-Dickinson methodology (Ingersoll et al., 1984).

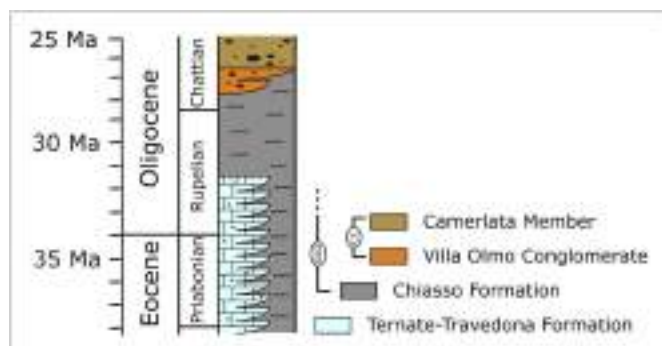


Fig. 2. Stratigraphy of the main foredeep deposits within the Adriatic foredeep system, according to Mancin et al. (2001) and Tremolada et al. (2010). GLG: Gonfolite Lombarda Group; CC: Como Conglomerate.

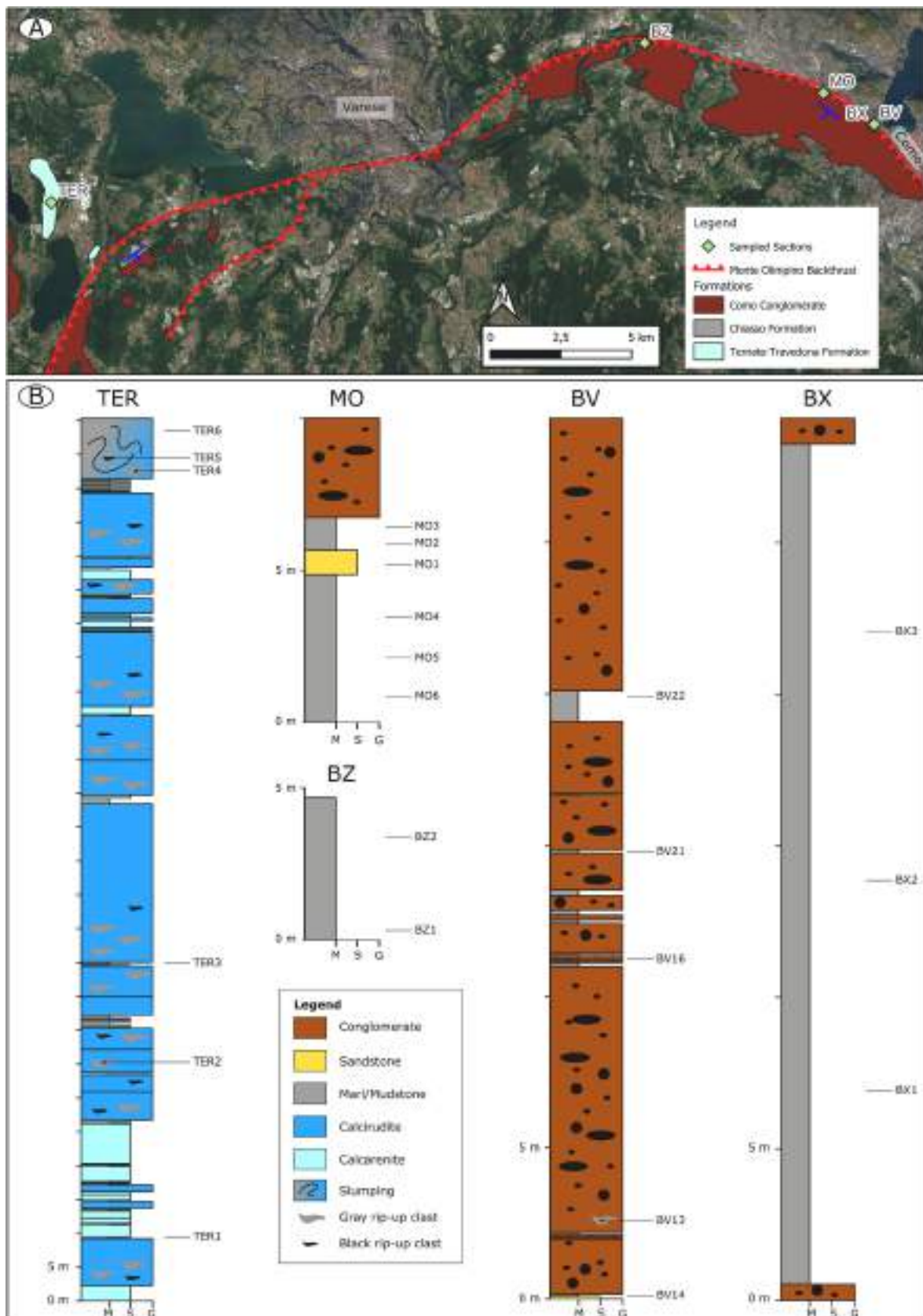


Fig. 3. A) location of the sequences sampled in this work (B).

4. Results

4.1. Ternate fm. (section TER)

In the Ternate-Travedona Formation, the sequence (named TER) is composed of thick bioclastic beds intercalated by fine-grained marly interbeds that were object of this work. The uppermost part of the sequence is closed up by a plurimetric-thick failure deposit (Figs. 3 and 4A and B). In addition, rip-up clasts pluricentimetric to pluridecimetric in length, light grey in colour and marly in composition, or dark grey with an orange to yellow coating, are widely included within all the sequence (Fig. 4C).

Marly interbeds (TER1 and TER3) show almost the same mineralogical association, mainly composed of calcite (56–72%), followed by minor amounts of quartz (18–13%), muscovite/illite (9%) and chlorite (6%) (e.g., Fig. 4D). Dolomite appears only in the lowermost studied layer (11%). Under the microscope (Fig. 4E), samples are predominantly composed of micrite mud, wrapping bioclastic fragments (mainly foraminifera and algae) and rare lithics of cherts, individuals of muscovite and quartz. Foraminifera association, present only in sample TER3, are characterized by the presence of taxa (*Globotruncana esnenhensis*) Campanian – Maastrichtian (Cretaceous) in age. On the contrary, calcareous nannofossil associations are characterized by Eocene/Oligocene long-range taxa that gave no attribution to a specific biozone.

The marly rip-up clast in the lower part of the sequence (TER2) is almost entirely composed of calcite (85%), with rare amounts of quartz (7%) and muscovite/illite (6%), and very rare amounts of chlorite (2%). Associations of both foraminifera taxa (*Globotruncanita stuarti*, *Globotruncana arca* - Campanian – Maastrichtian) and calcareous nannofossil taxa (*Micula murus* - upper Maastrichtian) point to a Cretaceous age.

Matrix within the failure deposit (TER6) shows a mineralogical composition similar to those of the marly interbeds: calcite (36%) and quartz (29%) dominate over muscovite/illite (16%) and chlorite (11%). Rare amounts of garnet (8%) were also documented. In thin section, micrite mud wraps rare individuals of quartz and muscovite. A reliable biostratigraphic attribution has been obtained for this layer through calcareous nannofossil association, characterized by common to rare *Isthmolithus recurvus*, *Discoaster barbadiensis*, and *D. saipanensis*, pointing to the Priabonian stage (NP19/20 biozones).

The sampled marly rip-up clast within this bed (TER4) is largely composed of quartz (54%), with minor amounts of clay minerals (montmorillonite) (13%), calcite (11%), dolomite (7%), and rare chlorite (3%). In addition, this sample is also characterized by the presence of plagioclase (7%), k-feldspar (3%) and garnet (2%). Foraminifera taxa associations (*Contusotruncana* sp., *Globotruncanita stuarti*, *Dentoglobigerina* sp.) date the sample to the Oligocene with good amounts of reworked Cretaceous taxa. Calcareous nannofossil content was barren.

The black rip-up clast (TER5) is almost entirely composed of barite, pyrite and oxides of cobalt and nickel. SEM-EDS analyses confirmed the presence of Fe, Ba, Co and Ni in combination with S and O (Fig. 4F and G).

4.2. Gonfolite Lombarda Group (BZ, MO, BV, BX sections)

Chiasso Formation and Villa Olmo Conglomerate have been sampled in four different sections, one in the Bizzarone (BZ) area and the other three (Monte Olimpino, Borgo Vico and Bixio sequences – MO, BV and BX from west to east) in the Como area. BZ and MO sections are composed of monotonous, homogenous fine-grained sediments, rarely interrupted by thin sandy layers (Fig. Figs. 3 and 5A and B). The BV sequence was previously described by Livio et al. (2011) and is composed of fine-grained muddy layers interbedded within thicker conglomerate beds. The BX sequence, exposed on top of the BV sequence, presents features similar to those of the BZ and the MO ones. All the sequences show similar compositions with quartz (22–54%) that dominates over all the other mineralogical components, which are

muscovite/illite (10–28%), plagioclase (13–24%), chlorite (7–20%), k-feldspar (3–12%), and rare dolomite (0–13%), calcite (0–12%) and pyroxene (6% in only one sample of the MO section). Clay minerals appear only in the uppermost part of section MO (4–6%). In thin section, samples from section BZ and BX are dominated by micrite mud wrapping individuals of muscovite, quartz and feldspars. In general, the siliciclastic fraction net increases in BV samples (Fig. 5C and D). No carbonate fragments have been observed in samples (see Table 1).

Point count carried out on the MO1 sample indicates a lithofeldspatho-quartzose composition (*sensu Garzanti, 2019*) for the sandstone layer, with a metamorphic index of 368 (*sensu Garzanti and Vezzoli, 2003*). Such sandstone chiefly consists of monocrystalline quartz, followed by plagioclase and K-feldspars. Micas are abundant (mostly 13% of detritus) and muscovite commonly prevails over brown micas. Few are the rock fragments (mainly medium-to high-rank felsic metamorphic lithics) (Fig. 5E and F; Table 2).

Calcareous nannofossils associations are generally poorly preserved with evident signs of dissolution and/or recrystallization, presence of few to rare cretaceous reworked taxa, and abundant inorganic clasts in all the sequences. On sixteen analysed samples, only three resulted useful for age constraints. One of them is at the bottom of the BZ sequence (BZ1), attributable to the NP24/25 biozones (*S. ciperoensis*). The other two samples are in the middle and upper part of the BX sequences, attributable respectively to the NP22/23 biozones (*S. predistentus*) (BX2) and to the NP24/25 biozones (*S. ciperoensis*) (BX3). No foraminifera were detected.

5. Discussions

5.1. Integrating the biostratigraphic constraints of the Paleogene Adriatic foredeep

Most of the recovered foraminifera and nannofossil associations gave low resolution age constraints or duplicate age constraints provided by previous works (e.g., Mancin et al., 2001; Tremolada et al., 2010). In other cases, they show clear old age constraints due to the presence of reworked taxa from Cretaceous sequences. Nevertheless, the uppermost layer of TER and BZ sections gave new remarkable age constraints on the evolution of sedimentary sequences within the basin.

The first of them is represented by the Oligocene age gain through foraminifera association in the failure deposit of TER section. Such age well supports the hypothesis of Mancin et al. (2001) that bioclastic sedimentation began in the Paleocene and lasted until the lower Oligocene (Rupelian), when the carbonate platform died, partially collapsing toward the basin. According to Coletti et al. (2016), such collapse was triggered by the drowning of the carbonate platform, therefore the present age constrains a major increase of the eustatic level during the Rupelian (lower Oligocene) in the Adriatic foredeep region.

The second age constraint is NP24/25 age recovered in the uppermost layer of the BZ sequence. Such attribution rejuvenates the Chiasso Formation – Villa Olmo Conglomerate boundary with respect of the previous NP 22/23 age of Gelati et al. (1988) in the central part of the basin. This is in line with the age of the same boundary further to the east in the Como area, where Tremolada et al. (2010) attribute the sequences studied in the present work at the NP24/25. Consequently, the NP22/NP23 attribution here obtained in the BX sequence must be considered as an effect of the presence of NP22/23 reworked taxa (*S. predistentus*) within the sequence, taxa commonly reworked also in the upper Gonfolite Lombarda Group at Como (Miocene – Tremolada et al., 2010). The NP24/25 biozones' attribution of the upper part of Chiasso Formation further to the west corroborates the hypothesis of a coeval activation of coarse-grained submarine systems within the Adriatic foredeep.

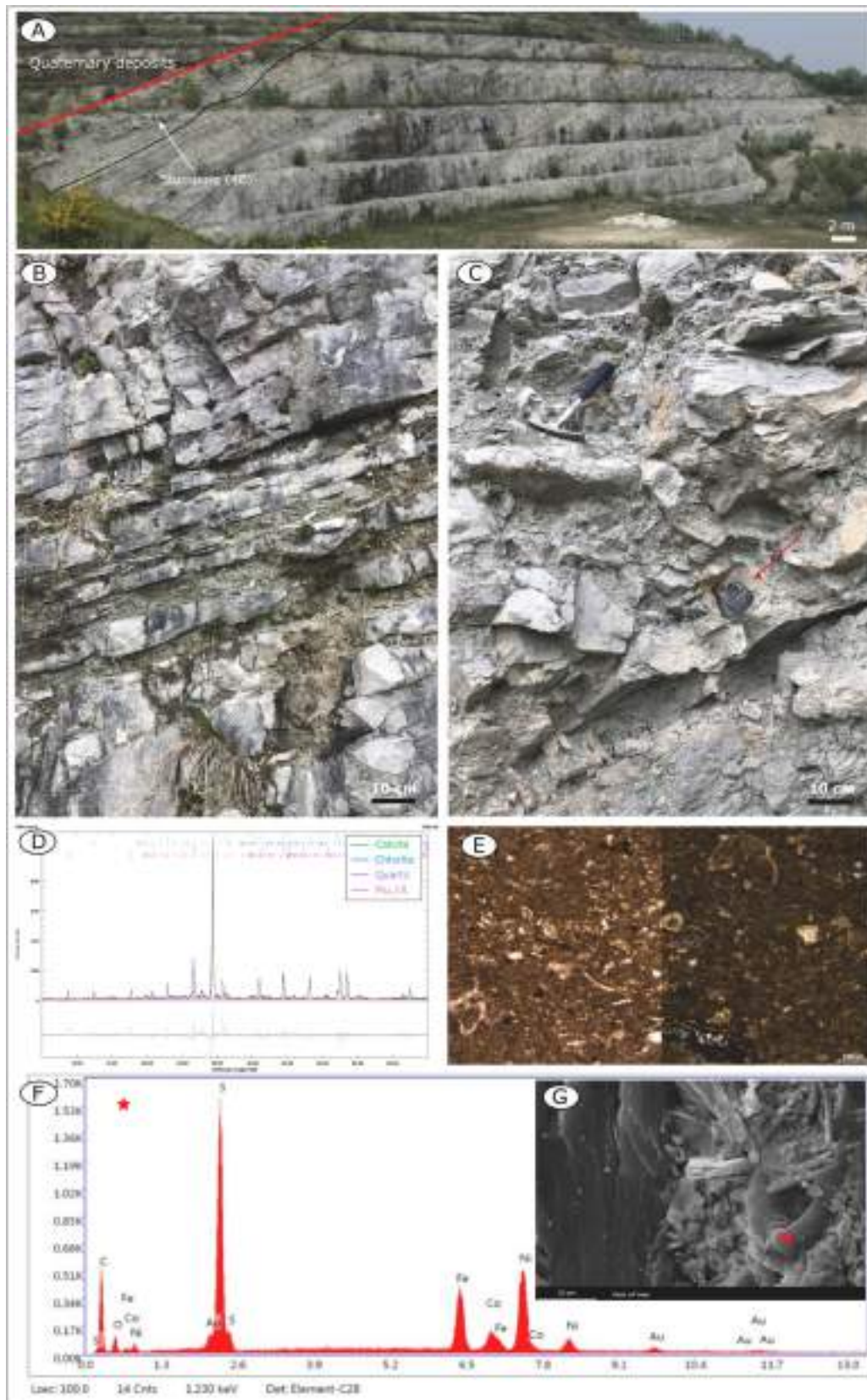


Fig. 4. A) field view of the TER sequence. B) Close-up view of calciturbidite layers interbedded by muddy layers. C) Field view of the slumping event closing the sedimentary sequence. The red arrow indicates one of the frequent black rip-up clast. D) XRD diagram of sample TER 1 (see Fig. 3 for location), showing calcite and quartz as main mineralogical phases, next to minor amounts of muscovite/illite and chlorite. E) Microphotographs of a muddy layer. Note the large amounts of foraminifera populating section. F) EDS analyses on Ni-, Co- and Fe-sulfur and oxides found black rip-up clasts as microcrystalline detritus (G).

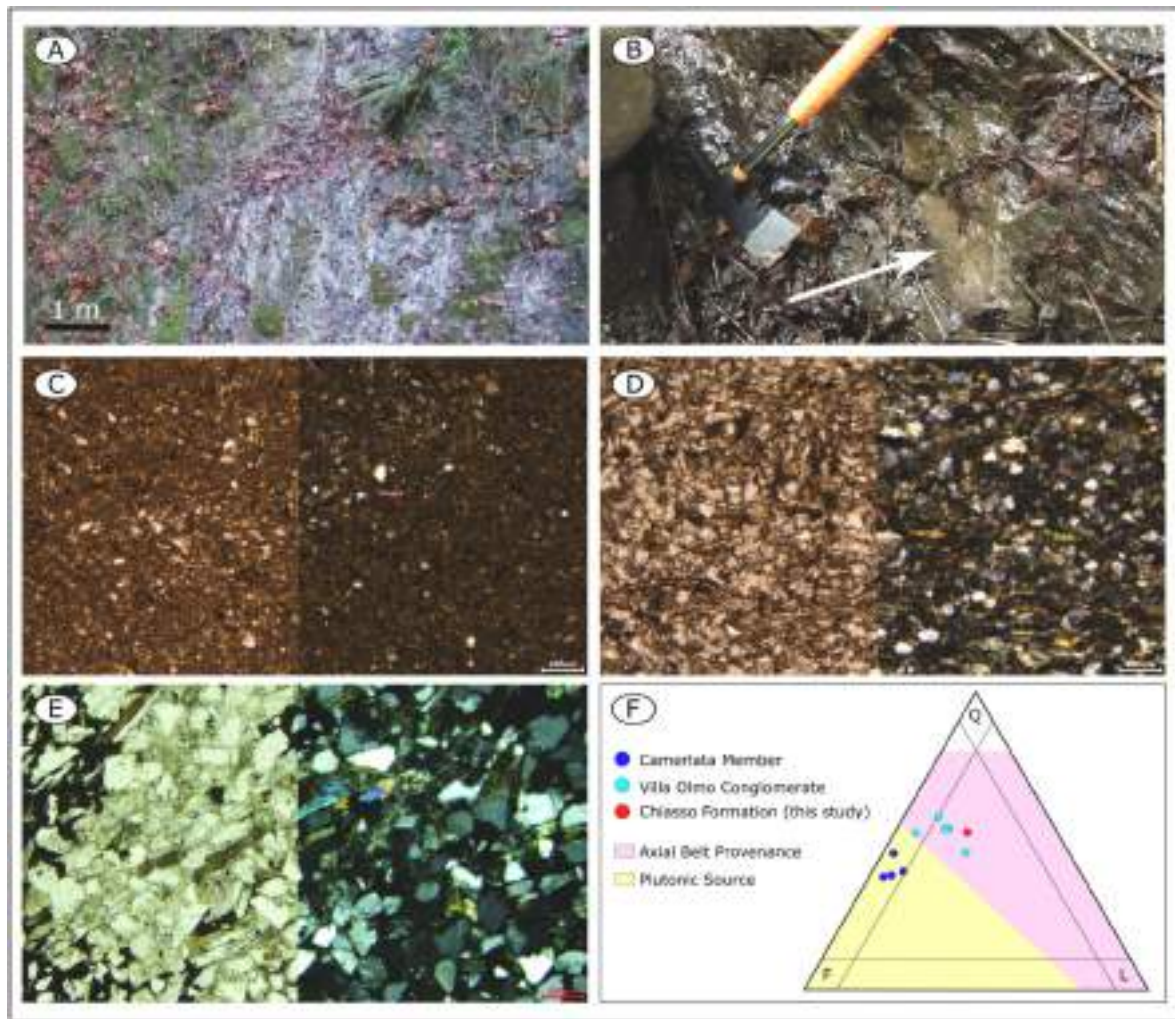


Fig. 5. A) typical outcrop of the Chiasso Formation, composed of thin, muddy layers, rarely interbedded by thin laminated sandstones (white arrow in Fig. 5B). C) Microphotograph of a muddy layer collected in the BZ section. D) Muddy layer within the BV section. D) Sandy layer of the MO section, showing a litho-feldspatho-quartzose composition, as shown in diagram (F). Axial belt provenance and Plutonic source are from Garzanti and Malusà (2008) and Coletti et al. (2016).

Table 1
Mineralogical compositions detected by XRD analysis.

| Sample | qtz | plg | kfs | chl | cal | dol | wm/ill | clay mins | barite | pyrox | grt |
|--------|-----|-----|-----|-----|-----|-----|--------|-----------|--------|-------|-----|
| BV13 | 30 | 18 | 3 | 7 | 10 | 7 | 25 | 0 | 0 | 0 | 0 |
| BV14 | 27 | 24 | 8 | 8 | 0 | 5 | 28 | 0 | 0 | 0 | 0 |
| BV16 | 54 | 20 | 7 | 9 | 0 | 0 | 10 | 0 | 0 | 0 | 0 |
| BV21 | 25 | 22 | 12 | 10 | 4 | 6 | 21 | 0 | 0 | 0 | 0 |
| BV22 | 34 | 17 | 4 | 14 | 7 | 0 | 24 | 0 | 0 | 0 | 0 |
| MO6 | 22 | 21 | 15 | 16 | 0 | 0 | 26 | 0 | 0 | 0 | 0 |
| MO5 | 35 | 15 | 9 | 12 | 0 | 8 | 21 | 0 | 0 | 0 | 0 |
| MO4 | 30 | 21 | 10 | 11 | 0 | 5 | 17 | 0 | 0 | 6 | 0 |
| MO1 | 23 | 23 | 9 | 11 | 5 | 0 | 25 | 4 | 0 | 0 | 0 |
| MO2 | 22 | 13 | 9 | 18 | 0 | 8 | 24 | 6 | 0 | 0 | 0 |
| MO3 | 28 | 18 | 6 | 20 | 0 | 0 | 23 | 5 | 0 | 0 | 0 |
| BZ1 | 25 | 18 | 7 | 10 | 12 | 11 | 17 | 0 | 0 | 0 | 0 |
| BZ2 | 39 | 13 | 4 | 12 | 5 | 13 | 14 | 0 | 0 | 0 | 0 |
| BX1 | 34 | 21 | 4 | 15 | 9 | 7 | 10 | 0 | 0 | 0 | 0 |
| BX2 | 25 | 17 | 10 | 12 | 12 | 10 | 14 | 0 | 0 | 0 | 0 |
| BX3 | 45 | 13 | 8 | 10 | 4 | 6 | 14 | 0 | 0 | 0 | 0 |
| TER1 | 18 | 0 | 0 | 6 | 56 | 11 | 9 | 0 | 0 | 0 | 0 |
| TER2 | 7 | 0 | 0 | 2 | 85 | 0 | 6 | 0 | 0 | 0 | 0 |
| TER3 | 13 | 0 | 0 | 6 | 72 | 0 | 9 | 0 | 0 | 0 | 0 |
| TER4 | 54 | 7 | 3 | 3 | 11 | 7 | 13 | 0 | 0 | 0 | 2 |
| TER6 | 29 | 0 | 0 | 11 | 36 | 0 | 16 | 0 | 0 | 0 | 8 |

Table 2

Key petrographic and mineralogical parameters of sandstone layer MO1 from the Chiasso Formation. Q = quartz; F = feldspar (KF = K-feldspar; P = plagioclase); L = lithic grains (Lv = volcanic; Lc = carbonate; Lph = shale/siltstone and chert; Lmsf = metasedimentary and metafelsite; Lmb = metabasite and ultramafic); HM = heavy minerals. MI* and MI = Metamorphic Indices (Garzanti and Vezzoli, 2003).

| FM | Sample | Q | KF | P | Lv | Lc | Lph | Lmsf | Lmb | mica | HM | total | MI* | MI |
|---------|--------|----|----|----|----|----|-----|------|-----|------|----|-------|-----|-----|
| Chiasso | MO1 | 55 | 9 | 18 | 2 | 0 | 0 | 3 | 0 | 13 | 0 | 100,0 | 368 | 280 |

5.2. Pale-drainages' reconstruction from the Eocene to the Oligocene

During the Eocene and the Lower Oligocene, provenance analyses on gravelly-sized detritus indicated that the Adriatic foredeep received inputs from the Mesozoic sediments proximal to the basin (Bernoulli et al., 1988; Mancin et al., 2001). Nevertheless, the largest part of the sedimentary sequences was constituted of marly to muddy detritus whose provenance has never been constrained, limiting the reconstruction of Alpine paleo-drainages before the Late Oligocene (e.g., Di Giulio et al., 2001; Garzanti and Malusà, 2008).

The compositional analyses on the terrigenous detrital fraction carried out in this work shed a new light on this point. Quartz, chlorite, muscovite and feldspars detected within the Ternate-Travedona Formation indicates that plutono-metamorphic terranes must have sourced detritus to the basin next to the Mesozoic sedimentary sequences during the Eocene and the Early Oligocene. The identification of garnet, a typical mineral index of medium to high-grade metamorphic rocks, and oxides and sulphurs of Co, Ni and Fe, typically deriving from the weathering of ultramafic rocks (Berger et al., 2011), allows a better identification of terranes involved in the sediment routing system, indicating a sediment source rooted within high-graded paraderived metamorphic terranes (garnet) and ultramafic terranes (oxides and sulfur of Co, Ni and Fe). In the Southern Alps, such kind of signature can be only found in the Diorite-Kinzigitte series of the Ivrea-Verbano complex that is composed, among the others, of paraderived and ultramafic terranes, the latter preserving Co and Ni oxides as weathering products (e.g., Mattioli et al., 1927; Carraro et al., 1970; Berger et al., 2012). This complex, already exposed to the surface during the Eocene (Berger et al., 2012), was (and is still) bordering the basin to the west and, therefore, largely supplied the quarzo-feldspathic detritus to the western Adriatic foredeep (Fig. 8A).

To the east, detrital signatures of muddy sediments of the Chiasso Formation (BZ and MO sections) are comparable to those of the Villa Olmo Conglomerate (BV and BX section), as their mineralogical assemblages do not show sensitive variations among each other. Such assemblages indicates that the paleo-drainage supplying this sector of the basin comprised the Permo-Mesozoic sedimentary covers of the Southalpine domain, which mostly include dolostones and limestones, interbedded by terrigenous formations, and spatially-limited volcanic sequences, together with the Southalpine metamorphic basements, which is mainly composed of para- and orthoderived terranes (e.g., Di Capua et al., 2016a). In addition, petrographic observations and calculated metamorphic index (368) for the MO1 sandy layer indicate an involvement of high-grade metamorphic terranes of the axial belt (terrane north of the PFS) (Garzanti et al., 2010), next to the aforementioned Southalpine domain terranes (Fig. 8B). This provenance is consistent with the presence of high-graded metamorphic detritus and plutonic detritus ascribable to the Bergell pluton and surrounding areas, documented within the Villa Olmo Conglomerate by several authors (e.g., Giger and Hurford, 1989; Carrapa and Di Giulio, 2001; Di Capua et al., 2016a, 2022).

5.3. Inherited tectonic setting and paleo-drainages evolution

The presence of ultramafic signature only in the western side of the basin represents a key point sustaining the hypothesis of a multiple drainage network feeding the Adriatic foredeep at the Eocene-Oligocene boundary. This period represents a turning point for the Southalpine belt

growth that passed from being a subduction-related, non-collisional orogen (Cretaceous – lower Paleogene) to a collisional orogen (upper Paleogene (e.g., Garzanti and Malusà, 2008; Zanchetta et al., 2015)). The control of this progressive geodynamic change on the evolution of surface network is recorded in the Cretaceous to Paleogene submarine sequences within the Adriatic foredeep. Considering the compositional data in the literature, it can be supposed that a multiple network of drainage systems was present in the area since the Cretaceous, with ultramafic detritus accumulation limited to the western side of the basin (within the Varese Flysch - Bernoulli and Winkler, 1990). This local signature and the subsequent multiple networks are then confirmed in the Paleogene, as documented in this work, and are well documented during the Oligo-Miocene boundary, as testified by the presence of ultramafic detritus in the westernmost outcrops belonging to the Como Conglomerate (Di Capua et al., 2022). Therefore, persistence of bimodal provenance from the Cretaceous to the Cenozoic times suggests that Southalpine drainage networks were already constituted during the Cretaceous subduction stage, in response to the first deformation of the Adriatic sequences, and then survived throughout the different phases of the orogenesis. Therefore, although it is impossible to identify pre-Neogene paleo-rivers compared to present-day topography, as no pre-Neogene terrestrial deposits connected to the basin are still preserved, it is likely that pre-Neogene drainage patterns developed exploiting Mesozoic tectonic lineaments as preferential ways through which drainages supplied sediments to the Adriatic foredeep (e.g., Di Capua et al., 2022). This would indicate that, during the collisional stage, rates at which paleo-drainages were acting on the topographic surface, denudating terranes and incising their pathways, were higher than tectonic deformation rates at which Southalpine sequences have been overturned towards south and southeast (e.g., Berger et al., 2012; Scaramuzzo et al., 2021). Persistence of detrital signatures were perturbed only when, with the activation of the dextral transpression along the Periadriatic Fault System during the post-collisional stage, Southalpine paleo-drainages were connected to drainage branches located to the north of the Periadriatic Fault system, beginning to receive detritus also from the Austroalpine and Penninic terranes across the Oligo-Miocene times (Carrapa and Di Giulio, 2001; Di Giulio et al., 2001; Malusà et al., 2011; Sciunnach, 2014; Di Capua et al., 2022).

5.4. Syn-sedimentary climate fingerprint on sediments' production and transportation

During the Eocene – Oligocene transition, Southern Alps and the related peripheral basins were in tropical to sub-tropical area, dominated by general wet climatic conditions that strongly influenced weathering of belt terranes and compositional signatures in basins' sediments (Mancin et al., 2001; Bassi and Nebelsick, 2010; Braga et al., 2010). Such conditions were at the base of the accumulation of Ni–Co oxides and sulfur revealed by SED-EDS analyses within the Ternate-Travedona Formation from one side, as well as at the base of the bias signature recorded by calcareous fragments within the sedimentary sequences on the other side. Ni–Co oxides and sulphurs are generally produced by weathering of ultramafic rocks under tropical-subtropical climate conditions (Berger et al., 2011). Their enrichment within the muddy detritus of the Ternate-Travedona Formation sequence indicates that large portions of ultramafic terranes were under strong weathering conditions, favoring the liberation of good volumes of Ni–Co oxides and sulphurs that underwent to transportation, dilution and accumulation

within the basin. In turn, carbonate grains are almost complete absent in mudstones (where the calcite signature of XRD is related to the precipitation of calcareous mud wrapping particles) and sandstones, but widely documented within conglomerates (Fig. 7) (cfr. Bernoulli et al., 1988; Carrapa and Di Giulio, 2001; Di Giulio et al., 2001; Bini et al., 2015; Di Capua et al., 2016a, 2022). This bias indicates that carbonate sequences, which constitute the Southalpine terrane belt most proximal to the basin, were subjected to strong weathering, being dissolved and transported by water in solution, rather than as particles by rivers. In turn, when large flash floods were discharged to the basin, carbonate fragments off-scraped from the substrate were mobilized together with other terrigenous materials and accumulated as debrites in the basin. This bias is relatable to the high proneness of carbonates to be weathered under wet tropical climatic conditions (e.g., Klunk et al., 2019; Goldscheider et al., 2020 and ref. therein), conditions that probably lasted across the considered time period.

Additional clues about how Paleogene climate was interacting with the belt is given by the presence of clay minerals. Clay minerals normally derive from the weathering of silicate rocks (e.g., Koita et al., 2013; Jaques et al., 2020), and dominate the Paleogene sedimentary sequences

of the Adriatic foredeep to the east (Bosellini and Trevisani, 1992) and to the south (Aldega et al.). Nevertheless, in the studied sequences, clay minerals abruptly appear only at the boundary between the Chiasso Formation and the Como Conglomerate, where calcite signal disappears from the deposits (Fig. 6). This sort of positive pulse of clay minerals (and negative pulse for calcite precipitation) might have been determined by a local change in climatic conditions, such as change in rainfall rates, or change in rainfall season alternation. Carbonates are normally more prone to weathering rather than silicates, but it has been demonstrated that under alternation of wet and dry seasons result in the alternation of weathering of carbonates and silicates differently, with the latter that are weathered instead of the first under dry climate (Tipper et al., 2006). Although few are the elements to gain to a conclusion in this work, it is possible to speculate that short term climatic trends recognized at the Rupelian/Chiattian boundary (e.g., Van Simaey et al., 2004 and ref. therein) had an influence on the production and transportation of sediments within the Adriatic foredeep, and such changes have been differently recorded from west to east of its margin. Combining these considerations with kinematic evolution of the belt (e.g., Berger et al., 2012; Scaramuzzo et al., 2022) would enhance models

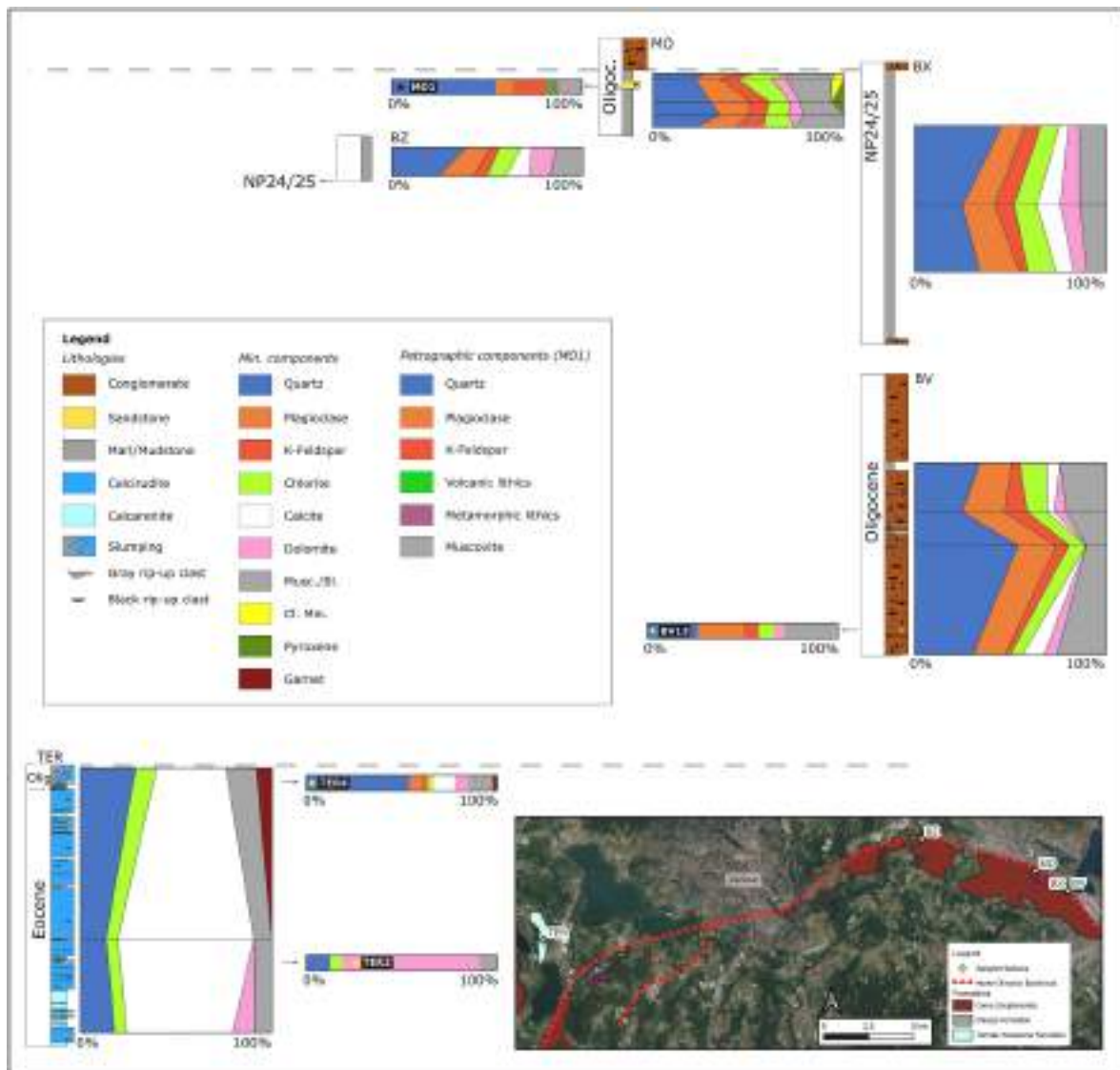


Fig. 6. Summary of petrographic, XRD and biostratigraphic results plotted on sampled logs. Diagrams on the right of the logs are results of XRD analyses, single plots are XRD and petrographic point count results on rip-up clasts (TER2, TER4, BV13) and a single sandy layer (MO1). Stratigraphic correlations are based on field evidence and previous works by Gelati et al. (1988), Tremolada et al. (2010) and Di Capua et al. (2016a,b). Musc./Ill.: muscovite/illite; Cl. Min.: clay minerals.



Fig. 7. Comparison among compositions of a sandy (S) layer, point-counted through Gazzi-Dickinson method, a muddy layer (M) through XRD analyses, and a conglomerate bed (C), gain through lithological association of the gravel-sized detritus (from Di Capua et al., 2016a,b) of section MO. Plu: plutonic rocks; And: andesites; mar: marls; par: paragneiss; rhy: rhyolites; ter: terrigenous; car: carbonate rocks; ort: ortogneiss; qtz: quartz; k-f: k-feldspar; dol: dolomite; clm: clay minerals; plg: plagioclase; chl: chlorite; w/i: muscovite/illite; Lv: volcanic lithics; Lm: metamorphic lithics; mu: muscovite.

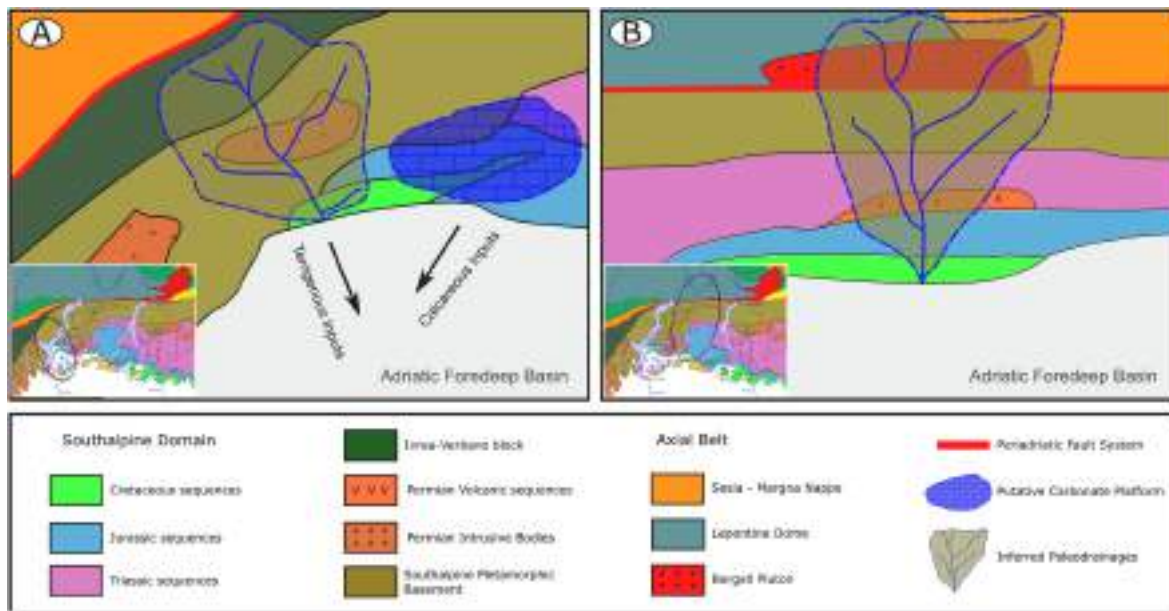


Fig. 8. Paleodrainages' sketches from provenance results. A) Paleodrainage supplying detritus to the Western Adriatic Foredeep Basin during the accumulation of the Ternate-Travedona Formation. Location of the Paleogene carbonate platform is only supposed. B) Paleodrainage supplying detritus to the eastern part of the Adriatic Foredeep Basin (Como area) during the accumulation of the Chiasso Formation.

on climatic feedbacks of the growth of the Alpine chain (e.g., Kuhlemann et al., 2002) and would give better constraints of how sedimentary mechanisms supplying detritus to a foredeep basin are controlled by tectonically-forced climate changes on millennial to millionaire time scale.

6. Conclusion

The application of analytical methodologies in the unravelling of provenance of fine-grained detritus has been greatly improved in the last two decades (e.g., Caracciolo et al., 2009, 2020; Perri et al., 2012;

Borromeo et al., 2019; Paleari et al., 2019; Cavalcante et al., 2023). In line with those Authors, the present work investigated the detrital signatures of fine-grained sequences accumulated from the Eocene to the Upper Oligocene in the north-western side of the Adriatic Foredeep basin. The multidisciplinary approach (mineralogical, petrographic and biostratigraphic analyses) within different stratigraphic levels of the sedimentary sequence allowed to enlarge the detrital source areas (once considered composed by the only Mesozoic Southalpine domain sequences), and revealed crucial information in the reconstruction of how sedimentary systems behave in transitional collisional to post-collisional geodynamic settings. The identification of an ultramafic signature only

within the western part of the basin documented the inheritance of source-to-sink system's paleo-drainages from the Alpine non-collisional stage of the Cretaceous time to that of the collisional stage of the Paleogene. The comparison between compositional data of fine and coarse detritus indicated a climatically controlled bias in sediment petrography, giving insights on putative changes in local climatic conditions that controlled sedimentary mechanisms supplying detritus to the foredeep basin.

Credit Author Statement

Andrea Di Capua: Conceptualization, Fieldwork, Petrographic analyses, Writing, Picture editing, Samuele Miano: Fieldwork, XRD analyses, SEM-EDS analyses, Franz A. Livio: Fieldwork, Writing, Picture editing, Giovanni Vezzoli: Petrographic analyses, Writing, Davide Campagnolo: XRD analyses, Alessandro Cavallo: XRD analyses, Writing, Gabriele Carugati: SEM-EDS analyses, Sergio Bonomo: Biostratigraphic analyses, Writing, Antonio Caruso: Biostratigraphic analyses, Writing, Davide Campagnolo: Writing.

Declaration of competing interest

The authors declare that they have no known competing financial interests or personal relationships that could have appeared to influence the work reported in this paper.

Data availability

Data will be made available on request.

Acknowledgments

Dr. Laura Galletti (Holcim) is acknowledged for sampling permission in the Ternate-Travedona Quarry. A. Berlusconi and G. Izzo are acknowledged for sampling assistance. The authors acknowledge four anonymous reviewers and the A.E. L. Caracciolo for their comments, which improved the early version of this manuscript.

References

- Aldega, L., Brandano, M., Cornacchia, I., Trophism, climate and paleoweathering conditions across the Eocene-Oligocene transition in the Massignano section (northern Apennines, Italy). *Sediment. Geol.* 405, 105701..
- Andò, S., Garzanti, E., 2014. Raman spectroscopy in heavy-mineral studies. *Geol. Soc., London, Special Publ.* 386 (1), 395–412.
- Bassi, D., Nebelsick, J.H., 2010. Components, facies and ramps: redefining upper Oligocene shallow water carbonates using coralline red algae and larger foraminifera (Venetian area, northeast Italy). *Palaeogeogr. Palaeoclimatol. Palaeoecol.* 295, 258–280.
- Berger, V.I., Singer, D.A., Bliss, J.D., Moring, B.C., 2011. Ni-Co Laterite Deposits of the World – Database and Grade and Tonnage Models. U.S. Geological Survey Open-File Report 2011-1058.
- Berger, A., Mercolli, I., Kapferer, N., Fügenschuh, B., 2012. Single and double exhumation of fault blocks in the internal sesia-lanzo zone and the ivrea-verbano zone (biella, Italy). *Int. J. Earth Sci.* 101, 1877–1894.
- Bernoulli, D., Winkler, W., 1990. Heavy mineral assemblages from Upper Cretaceous South- and Austroalpine flysch sequences (Northern Italy and Southern Switzerland): source terranes and paleotectonic implications. *Eclogae Geol. Helv.* 83, 287–310.
- Bernoulli, D., Herb, R., Gröning, A., 1988. Ternate Formation, a late Eocene bioclastic submarine fan of the lombardian basin (southern Alps). *Am. Petrol. Geol. Bull.* 72, 988.
- Bernoulli, D., Giger, M., Müller, D.W., Ziegler, U.R.F., 1993. Sr-isotope-stratigraphy of the gonfolite Lombarda Group ("South-Alpine molassa". northern Italy) and radiometric constraints for its age of deposition. *Eclogae Geol. Helv.* 86, 751–767.
- Bersezio, R., Fornaciari, M., Gelati, R., Napolitano, A., Valdisturlo, A., 1993. The significance of the Upper Cretaceous to Miocene clastic wedges in the deformation history of the Lombardian southern Alps. *Geol. Alpina* 69, 3–20.
- Bini, A., Scunnach, D., Bersezio, R., Scardia, G., Tomasi, F., 2015. Note Illustrative Alla Carta Geologica d'Italia Alla Scala 1:50000, Foglio 096 Seregno.
- Borromeo, L., Andò, S., France-Lanord, C., Coletti, G., Hahn, A., Garzanti, E., 2019. Provenance of bengal shelf sediments: 1. Mineralogy and geochemistry of silt. *Minerals* 9 (10), 640.
- Bown, P.R., Lees, J.A., Young, J.R., 2004. Calcareous nannoplankton evolution and diversity through time. In: Thierstein, H.R., Young, J.R. (Eds.), *Coccolithophores - from Molecular Processes to Global Impact*. Springer, Berlin, pp. 481–508.
- Braga, J.C., Bassi, D., Piller, W.E., 2010. Palaeoenvironmental significance of Oligocene-Miocene coralline red algae – a review. *Int. Assoc. Sedimentol. Spec. Publ.* 42, 165–182.
- Caracciolo, L., Andò, S., Vermeesch, P., Garzanti, E., McCabe, R., Barbarano, M., Paleari, C., Rittner, M., Pearce, T., 2020. A multidisciplinary approach for the quantitative provenance analysis of siltstone: Mesozoic Mandawa Basin, southeastern Tanzania. In: *Application of Analytical Techniques to Petroleum Systems*. Dowey, Osborne and Volk, vol. 484. The Geological Society of London Special Publication.
- Carrapa, B., Di Giulio, A., 2001. The sedimentary record of the exhumation of a granitic intrusion into a collisional setting: the lower Gonfolite Lombarda Group, Southern Alps, Italy. *Sediment. Geol.* 139, 217–228.
- Carraro, F., Dal Piaz, G.V., Sacchi, R., 1970. Serie di Valpelle e il zona dioritico-kinzigitica sono i relitti di un ricoprimento proveniente dalla Zona Ivrea-Verbano. *Memor. Soc. Geol. Ital.* 2, 197–224.
- Cita, M.B., 1957. Sintesi stratigrafica della "Gonfolite". *Riv. Ital. Paleontol. Stratigr.* 63, 79–117.
- Cavalcante, F., Perri, F., Belviso, C., Lettino, A., Prosser, G., La Bruna, V., Agosta, F., 2023. Clayey sediments analysis as a useful tool to assessing the geodynamic evolution of fold-and-thrust belts: The case study of the Monte Alpi area (northern Apennines, Italy). *Mar. Petrol. Geol.* 151, 106204. <https://doi.org/10.1016/j.marpetgeo.2023.106204>.
- Chipera, S.J., Bish, D.L., 2002. FULLPAT: a full-pattern quantitative analysis program for X-ray powder diffraction using measured and calculated patterns. *J. Appl. Crystallogr.* 35 (6), 744–749. <https://doi.org/10.1107/S0021889802017405>.
- Coletti, G., Vezzoli, G., Di Capua, A., Basso, D., 2016. Reconstruction of a lost carbonate factory based on its biogenic detritus (Ternate-Travedona Formation and gonfolite Lombarda Group – northern Italy). *Res. Paleontol. Stratigraphy* 122 (3), 1–22.
- DeCelles, P.G., 1988. Lithologic provenance modelling applied to the Late Cretaceous synorogenic Echo Canyon Conglomerate, Utah: a case of multiple source areas. *Geology* 16, 1039–1043.
- Di Capua, A., Vezzoli, G., Cavallo, A., Groppelli, G., 2016a. Clastic sedimentation in the Late Oligocene Southalpine Foredeep: from tectonically driven melting to tectonically driven erosion. *Geol. J.* 51, 338–353.
- Di Capua, A., Vezzoli, G., Groppelli, G., 2016b. Climatic, tectonic and volcanic controls of sediment supply to an Oligocene Foredeep basin: the val d'Aveto formation (northern Italian apennines). *Sediment. Geol.* 332, 68–84.
- Di Capua, A., Pandini, R., Barilaro, F., Cavallo, A., Livio, F.A., 2022. Drainage pattern evolution during continental indentation in Central Alps: constraints from the sedimentary record of associated deep-water offshoots. *Mar. Petrol. Geol.* 144, 105846.
- Di Giulio, A., Carrapa, B., Fantoni, R., Gorla, L., Valdisturlo, A., 2001. Middle Eocene to early Miocene sedimentary evolution of the western lombardian segment of the South alpine foredeep (Italy). *Int. J. Earth Sci.* 90, 534–548.
- Garzanti, E., 2019. Petrographic classification of sand sandstone. *Earth Sci. Rev.* 192, 545–563.
- Garzanti, E., Vezzoli, G., 2003. A classification of metamorphic grains in sands based on their composition and grade. *J. Sediment. Res.* 73, 830–837.
- Garzanti, E., Malusà, M.G., 2008. The Oligocene Alps: domal unroofing and drainage development during early orogenic growth. *Earth Planet Sci. Lett.* 268, 487–500.
- Gelati, R., Napolitano, A., Valdisturlo, A., 1988. La "Gonfolite Lombarda": stratigrafia e significato nell'evoluzione del margine sudalpino. *Riv. Ital. Paleontol. Stratigr.* 94, 285–332.
- Goldscheider, N., Chen, Z., Auler, A.S., Bakalowicz, M., Broda, S., Drew, S., Hartmann, J., Jiang, G., Moosdorf, N., Stevanovic, Z., Veni, G., 2020. Global distribution of carbonate rocks and karst water resources. *Hydrogeol. J.* 28, 1661–1677.
- Ingersoll, R.V., Bullard, T.F., Ford, R.L., Grimm, J.P., Pickle, J.D., Sares, S.W., 1984. The effects of grain size on detrital modes: a test of the Gazzi-Dickinson point-counting method. *J. Sediment. Petrol.* 54, 103–116.
- Jaques, D.S., Marques, E.A.G., Marcellino, L.C., Leão, M.F., Ferreira, E.P.S., dos Santos Lemos, C.C., 2020. Changes in the physical, mineralogical and geomechanical properties of a granitic rock from weathering zones in a tropical climate. *Rock Mech. Rock Eng.* 53, 5345–5370.
- Klunk, M.A., Dasgupta, S., Das, M., Wander, P.R., Di Capua, A., 2019. Geochemical speciation and batch mode simulation in the carbonate depositional environments. *Periódico Tche Química* 16 (133).
- Koita, M., Jourde, H., Koffi, K.J.P., Da Silveira, K.S., Biao, A., 2013. Characterization of weathering profile in granites and volcanosedimentary rocks in West Africa under humid tropical climate conditions. Case of the Dimbokro Catchment (Ivory Coast). *J. Earth Syst. Sci.* 122, 841–854.
- Kuhlemann, J., Frisch, W., Székely, B., Dunkl, I., Kázmér, M., 2002. Post-collisional sediment budget history of the Alps: tectonic versus climatic control. *Int. J. Earth Sci.* 91, 818–837.
- Litty, C., Schlunegger, F., 2017. Controls on pebbles' size and shape in streams of the Swiss Alps. *J. Geol.* 125, 101–112.
- Lu, G., Di Capua, A., Winkler, W., Rahn, M., Guillong, M., von Quadt, A., Willet, S.D., 2019. Restoring the source-to-sink relationships in the Paleogene foreland basins in the Central and Southern Alps (Switzerland, Italy, France): a detrital zircon study approach. *Int. J. Earth Sci.* 108, 1817–1834.
- Lu, G., Fellin, M.G., Winkler, W., Rahn, M., Guillong, M., von Quadt, A., Willet, S.D., 2020. Revealing exhumation of the central Alps during the Early Oligocene by detrital zircon U-Pb age and fission track double dating in the Tavayannaz Formation. *Int. J. Earth Sci.* 109, 2425–2446.

- Malusà, M.G., Villa, I.M., Vezzoli, G., Garzanti, E., 2011. Detrital geochronology of unroofing magmatic complexes and the slow erosion of Oligocene volcanoes in the Alps. *Earth Planet Sci. Lett.* 301, 324–336.
- Mancin, N., Ceriani, A., Tagni, F., Brambilla, G., 2001. La Formazione di Ternate (Italia settentrionale): contenuto micropaleontologico e caratterizzazione petrografica. *Atti Ticinesi di Scienze della Terra* 42, 37–46.
- Martini, E., 1971. Standard Tertiary and Quaternary calcareous nannoplankton zonation. In: *Tecnosci (Ed.), Proceedings 2nd International Conference Planktonic Microfossils* Roma, vol. 2, pp. 739–785.
- Mattirolo, E., Novarese, V., Franchi, S., Stella, A., 1927. Carta Geologica d'Italia Alla Scala 1: 100.000, Foglio 30 "Varallo". Regio Ufficio Geologico.
- Okada, H., Bukry, D., 1980. Supplementary modification and introduction of code numbers to the low-latitude coccolith biostratigraphy. *Mar. Micropaleontol.* 5, 321–325.
- Paleari, C.I., Delmonte, B., Andò, S., Garzanti, E., Petit, J.R., Maggi, V., 2019. Aeolian dust provenance in central East Antarctica during the Holocene: environmental constraints from single-grain Raman spectroscopy. *Geophys. Res. Lett.* 46 (16), 9968–9979.
- Perch-Nielsen, K., 1985. Cenozoic calcareous nannofossils. In: *Bolli, H.M., Saunders, J.B., Perch-Nielsen, K. (Eds.), Plankton Stratigraphy*. Cambridge University Press, Cambridge, pp. 427–554.
- Perri, F., Critelli, S., Dominici, R., Muto, F., Tripodi, V., Ceramicola, S., 2012. Provenance and accommodation pathways of late Quaternary sediments in the deep-water northern Ionian Basin, southern Italy. *Sedimentary Geology* 280, 244–259.
- Premoli Silva, I., Tremolada, F., Sciunnach, D., Scardia, G., 2010. Aggiornamenti biocronologici e nuove interpretazioni ambientali sul Paleocene-Eocene della Brianza (Lombardia). In: *Orombelli, G., Cassinis, G., Gaetani, M. (Eds.), Una nuova geologia per la Lombardia*, Accademia di Scienze e Lettere Incontri di Studio, 54. Istituto Lombardo, pp. 141–160.
- Scaramuzzo, E., Livio, F.A., Granado, P., Di Capua, A., Bitonte, R., 2022. Anatomy and kinematic evolution of an ancient passive margin involved into an orogenic wedge (Western Southern Alps, Varese area, Italy and Switzerland). *Swiss J. Geosci.* 115 (4), 1–21.
- Sciunnach, D., 2014. Geochemistry of detrital chromian spinel as a marker for cenozoic multistage tectonic evolution of the Alps. *Rendiconti Online della Società Geologica Italiana* 32, 15–23.
- Tremolada, F., Guasti, E., Scardia, G., Carcano, C., Rogledi, S., Sciunnach, D., 2010. Reassessing the biostratigraphy and the paleobathymetry of the gonfolite Lombarda Group in the Como area (northern Italy). *Riv. Ital. Paleontol. Stratigr.* 116, 35–49.
- Van Simaey, S., De Man, E., Vandenberghe, N., Brinkhuis, H., Steurbaut, E., 2004. Stratigraphic and palaeoenvironmental analysis of the Rupelian–Chattian transition in the type region: evidence from dinoflagellate cysts, foraminifera and calcareous nannofossils. *Palaeogeogr. Palaeoclimatol. Palaeoecol.* 208, 31–58.
- Zanchetta, S., Malusà, M.G., Zanchi, A., 2015. Precollisional development and cenozoic evolution of the southalpine retrobelt (European Alps). *Lithosphere* 7, 662–681.